Chemosphere 344 (2023) 140380

Contents lists available at ScienceDirect

Chemosphere

journal homepage: www.elsevier.com/locate/chemosphere

Perfluoroalkyl substances exposure alters stomatal opening and xylem hydraulics in willow plants

Ilaria Battisti [a,1,*], Dario Zambonini [b,1], Leonard Barnabas Ebinezer [a], Anna Rita Trentin [a], Franco Meggio [a], Giai Petit [b], Antonio Masi [a]

[a] Department of Agronomy, Food, Natural Resources, Animals and Environment (DAFNAE), University of Padova, Viale dell'Università 16, Legnaro, PD, Italy
[b] Department of Land, Environment, Agriculture and Forestry (TESAF), University of Padova, Viale dell'Università 16, Legnaro, PD, Italy

HIGHLIGHTS

- PFAS accumulation in plant tissues depends on their chemical properties.
- Short-chain PFAS accumulates in *Salix* stems.
- PFAS-exposed plants have reduced stomatal conductance.
- Reduced stomatal conductance is abscisic acid and salicylic acid independent.
- PFAS-treated plants are more vulnerable to xylem cavitation.

GRAPHICAL ABSTRACT

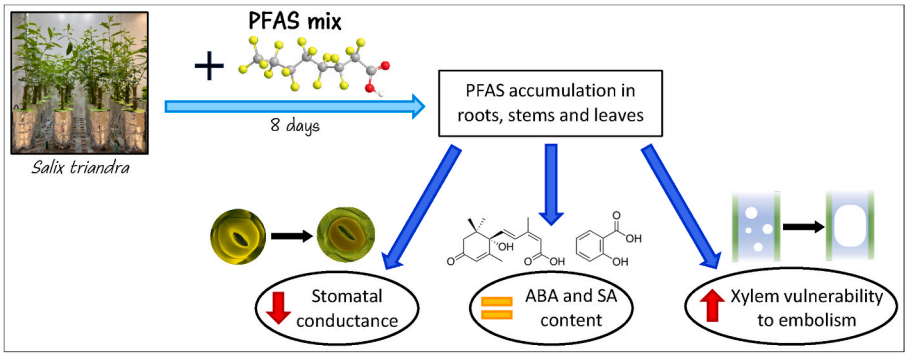

ARTICLE INFO

Handling Editor. Magali Houde

Keywords:
PFAS
Persistent organic pollutants
Stomata
Xylem vulnerability
Embolism
Water balance

ABSTRACT

Climate change and pollution are increasingly important stress factors for life on Earth. Dispersal of poly- and perfluoroalkyl substances (PFAS) are causing worldwide contamination of soils and water tables. PFAS are partially hydrophobic and can easily bioaccumulate in living organisms, causing metabolic alterations. Different plant species can uptake large amounts of PFAS, but little is known about its consequences for the plant water relation and other physiological processes, especially in woody plants. In this study, we investigated the fractionation of PFAS bioaccumulation from roots to leaves and its effects on the conductive elements of willow plants. Additionally, we focused on the stomal opening and the phytohormonal content. For this purpose, willow cuttings were exposed to a mixture of 11 PFAS compounds and the uptake was evaluated by LC-MS/MS. Stomatal conductance was measured and the xylem vulnerability to air embolism was tested and further, the abscisic acid and salicylic acid contents were quantified using LC-MS/MS. PFAS accumulated from roots to leaves based on their chemical structure. PFAS-exposed plants showed reduced stomatal conductance, while no differences were observed in abscisic acid and salicylic acid contents. Interestingly, PFAS exposure caused a higher vulnerability to drought-induced xylem embolism in treated plants. Our study provides novel information about the PFAS effects on the xylem hydraulics, suggesting that the plant water balance may be affected by PFAS exposure. In

* Corresponding author.
E-mail addresses: ilaria.battisti@studenti.unipd.it, ilaria.battisti@unipd.it (I. Battisti).
[1] These authors equally contributed to this work.

https://doi.org/10.1016/j.chemosphere.2023.140380
Received 18 July 2023; Received in revised form 4 October 2023; Accepted 5 October 2023
Available online 7 October 2023

this perspective, drought events may be more stressful for PFAS-exposed plants, thus reducing their potential for phytoremediation.

1. Introduction

Natural ecosystems including plants are exposed to different types of anthropogenic stresses, such as fossil fuel emissions, deforestation, and extensive unplanned land use. Increasing atmospheric carbon, consequently leads to warmer global temperatures that are raising the frequency of extreme events, like heat waves and drought conditions (Cook et al., 2018; Marx et al., 2021). Such conditions are some of the major limitations to plant health and this may be exacerbated by environmental pollution, which can affect the plant physiology at different levels (Darrall, 1989; Rai, 2016).

In recent years, there are rising concerns worldwide about the ubiquitous presence of poly- and perfluoroalkyl substances (PFAS) in the environment and its impact on human health and the natural ecosystem. PFAS are a large family of synthetic compounds, whose chemical structure provides amphiphilic properties, as well as high chemical and thermal stability (Wang et al., 2020a), making them extremely persistent in the environment and resistant to degradation. Due to their unique properties, PFAS are intensely used in the industry, and their subsequent discharge leads to the global occurrence of PFAS in the environment and biota (Li et al., 2022). PFAS have been detected in numerous environmental matrices, such as air, water, sediment, and sludge (Zhang et al., 2020). These compounds are highly bioaccumulative and several studies reported PFAS to be present in human tissues (Pérez et al., 2013) and plants (Wang et al., 2020b, 2020a; Zhou et al., 2021). Multiple epidemiological studies found significant association between PFAS exposure and adverse effects on human health (Sunderland et al., 2019; Fenton et al., 2021). Therefore, the environmental prevalence and potential toxicity of PFAS raise alarming concerns about risks to human health, as ingestion of contaminated drinking water and food, inhalation of polluted air and contact with contaminated media represent the primary PFAS exposure routes for animals and humans (Sunderland et al., 2019). PFAS accumulation has been widely reported in agricultural crops (Ghisi et al., 2019; Lesmeister et al., 2021), thus fruits and vegetables grown in a polluted environment are a potential source of PFAS intake.

PFAS toxicity in plants has been widely investigated, mostly at very high concentrations not reported in the environment. PFAS concentration at mM range was shown to be phytotoxic and inhibited growth parameters such as germination rate, biomass, root length, height, leaf number. PFAS are usually reported at ng L^{-1} levels in water and ng g^{-1} levels in soil and hence, studies with PFAS concentration in this range are more environmentally relevant (Li et al., 2022; Adu et al., 2023). Nevertheless, the effects have been evaluated at the physiological, biochemical and molecular levels. PFAS have been demonstrated to affect phenotype, cell morphology and photosynthetic activity, to increase oxidative stress and enzymatic antioxidant activity, and to alter the expression of genes and proteins involved in oxidative stress and photosynthesis (Li et al., 2022; Adu et al., 2023). Moreover, PFAS exposure is known to alter the content of metabolites, such as phytohormones, amino acids, fatty acids, and polyphenols even though no phytotoxic effects were evident morphologically (Li et al., 2022; Adu et al., 2023). Research on PFAS accumulation and effects has been mostly carried out on model organisms or crop plants (Yang et al., 2015; Xu et al., 2022). Although a similar trend in PFAS accumulation in plants can be observed, there is a noticeable disparity in terms of phytotoxicity and bioaccumulation across different crops. Also, this seems to vary when exposed to a single or a combination of PFAS, the carbon chain length, functional group, and the concentration used. Factors such as protein and lipid content in roots, pH, temperature and soil organic carbon also is known to influence PFAS bioaccumulation (Adu et al., 2023). Hence, bioaccumulation and phytotoxicity data obtained with crops may not be comparable with other crops and plants, especially in woody plants and trees, wherein the information in terms of PFAS bioaccumulation and phytotoxicity is comparatively scant.

Some wetland plants and woody terrestrial plants may represent a potential solution for PFAS phytomanagement, given their high bioaccumulation and translocation capacity (Huff et al., 2020; Wang et al., 2020b; Evangelou and Robinson, 2022). Among woody plants, *Salix* species are fast-growing trees that are known for their ability to grow in a variety of environmental conditions, including wetland areas and riverbanks. Previous studies have highlighted their capability to accumulate PFAS, with not much drastic impact on growth (Sharma et al., 2020; Würth et al., 2023), however, other possible subtle yet important physiological impairments due to PFAS accumulation in these plants are yet to be investigated and hence, cannot be ruled out.

Water movement in plants includes i) passing of the root epidermis barrier and crossing the Casparian band, ii) cohesion and adhesion of water molecules into the conductive elements, and iii) driven by a negative water potential, movement up to the sub-stomatal cavity in the leaf, and iv) finally evaporation through the stomata opening. Water moves from roots to leaves along a gradient of negative water potential generated by the water evaporating from the cell walls of the leaf mesophyll cells. High leaf transpiration rates triggered by high vapor pressure deficits in the atmosphere and/or low soil water availability can determine a reduction in xylem water potential below a critical point (Grossiord et al., 2020). Gas bubbles dissolved in water can thus expand and occupy the whole volume of certain vascular elements making them dysfunctional for water transport (Cochard, 2006), i.e., embolisms lead to losses of xylem hydraulic conductance. The xylem vulnerability to embolism formation (i.e., the % of conductance lost at a given water potential) is correlated with several anatomical traits (e.g., pit membrane porosity) and biochemical properties of the xylem tissue (Lens et al., 2022), and with the biochemical composition of the circulating sap (Nardini et al., 2011). Widespread embolism formation in xylem conduits can thus limit leaf water supply, leading to a reduction in leaf gas exchange, and ultimately plant desiccation and death (Barigah et al., 2013). Factors altering any of these aspects, including the formation of air emboli in xylem conduits, will affect the long-distance water translocation across the vascular tissue.

PFAS substances can move without much sorption across water in a hydroponic experimental setup and hence, they may readily translocate through the xylem to all plant tissues. PFAS occurrence in the xylem of the stem was recently demonstrated by Wang et al. (2020b). Due to their sticky nature, it is highly likely that PFAS may adhere to the lignocellulosic matrix constituting the xylem vessels (Vasić et al., 2023), thus altering their hydrophilicity and affecting the water molecules' adhesion to the xylem conduits, ultimately altering the xylem embolism vulnerability.

Based on these considerations, we hypothesized that PFAS taken up by the roots would adhere and accumulate also in the stem (xylem vessels) of plants and this could negatively affect xylem conductivity, causing detrimental effects on plant physiology. To the best of our knowledge, the impact of PFAS accumulation on xylem hydraulic conductivity has not been examined yet. In this work, we aimed to investigate this aspect in woody *Salix triandra* plants hydroponically grown in a PFAS-spiked nutrient solution. Although PFAS in the environment are predominantly reported as a mixture, it is not yet fully understood if and how each PFAS affects the translocation and accumulation of other PFAS in plants. In the present study, we used a combination of 11 different PFAS, representative of the carbon chain length and functional groups, and at a concentration range usually detected in polluted areas (Ahrens, 2011; Valsecchi et al., 2015; Wang et al., 2019).

2. Materials and methods

2.1. Chemicals

PFAS included in the experiment are: perfluorobutanoic acid (PFBA), perfluorobutane sulfonate (PFBS), perfluoropentanoic acid (PFPeA), perfluorohexanoic acid (PFHxA), perfluoroheptanoic acid (PFHpA), perfluorooctanoic acid (PFOA), perfluorooctane sulfonate (PFOS), perfluorononanoic acid (PFNA), perfluorodecanoic acid (PFDA), perfluoroundecanoic acid (PFUnA) and perfluorododecanoic acid (PFDoA) (Sigma Aldrich, USA). Identification and quantification of all PFAS were performed using the isotopically-labeled PFAS standards ($^{13}C_4$-PFBA, $^{13}C_3$-PFBS, $^{13}C_5$-PFPeA, $^{13}C_5$-PFHxA, $^{13}C_4$-PFHpA, $^{13}C_8$-PFOA, $^{13}C_8$-PFOS, $^{13}C_9$-PFNA, $^{13}C_6$-PFDA, $^{13}C_7$-PFUnA, $^{13}C_2$-PFDoA, Wellington Laboratories, Canada) added at a fixed concentration as internal standards in mass spectrometry analysis. Phytohormones standards (abscisic acid - ABA, salicylic acid - SA) were purchased from OlChemIm s.r.o. (Czech Republic).

2.2. Plant growth and treatment

Willow cuttings (*Salix triandra*, ~35 cm in length) collected from the Plant Biodiversity and Agroforestry Center of Veneto Agricoltura, (Montecchio Precalcino, Vicenza, Italy), were hydroponically grown in greenhouse conditions, initially in water for 12 days, then in half-strength modified Hoagland nutrient solution (Hoagland, 1933) for 3 days and finally in full strength nutrient solution. After rooting and shooting, 66 plants were selected for uniformity and transferred to single plastic pots and moved to a growth chamber (12/12 h light/dark period, 25/20 °C temperature and 300 μmol photons m^{-2} s^{-1} of photosynthetic active radiation, PAR). After 3 days of adaption, plants were equally divided into two groups and treated for 8 days as described by Sharma et al. (2020) with a PFAS mixture each one at 100 μg L^{-1}. The PFAS-spiked nutrient solution was analyzed as described below prior to starting the plant treatment to verify the PFAS content.

2.3. PFAS sampling, extraction and quantification by LC-MS/MS analysis

An aliquot of fresh leaves for each plant was instantly frozen with liquid nitrogen and stored at −20 °C until phytohormones extraction. The uptake of PFAS was monitored in terms of depletion from the nutrient solution at the end of the treatment: 1 mL of nutrient solution was collected and filtered with 0.22 μm cellulose acetate (CA) membranes and stored at 4 °C until LC-MS/MS analysis.

PFAS in root and leaf samples, collected at the end of the experimental period, were extracted using an accelerated solvent extraction (ASE) system (Dionex ASE 350, Thermo Fisher Scientific, USA). Prior to extraction, samples were dried, ground into fine powder and pulled to create 18 replicates. For each replicate, 0.1 g and 0.2 g of roots and leaves powder, respectively, underwent ASE extraction. The ASE operated at 125 °C and 9.0–10.3 MPa, using methanol as solvent. Extracts were then filtered using 0.22 μm CA membranes and stored at 4 °C until LC-MS/MS analysis.

PFAS content in wood was determined for samples used for xylem cavitation experiments (see paragraph 2.9). Stems were cut into thick slices and ground into fine powder, prior to ASE extraction. For each replicate, 0.5 g of wood powder was extracted and filtered using the method described above.

The amount of PFAS in nutrient solution, roots, leaves and wood samples was measured by LC-MS/MS using a triple quadrupole (TSQ Quantiva, Thermo Fisher Scientific, USA) coupled to an ultra-high performance liquid chromatography (Ultimate 3000 UHPLC, Dionex, Thermo Fisher Scientific, USA). The chromatographic method and mass spectrometer conditions are reported in detail by Sharma et al. (2020). Before the analysis, ^{13}C PFAS internal standard mixture (Wellington Laboratories, Canada) was added to each sample at 2 μg L^{-1} final concentration. Nutrient solution samples were diluted 1:10 with water before analysis. Roots and leaves samples were diluted 1:1 with H_2O prior to injection. Data acquisition was performed in selected reaction monitoring mode (SRM, see Table S1 for optimized parameters), and raw files were processed with Skyline MS software v. 21.2.0.425 (Adams et al., 2020).

2.4. Quality control and quality assurance

Glass containers and all materials potentially containing per- or polyfluorinated polymers were avoided to prevent background contamination, and carry over was monitored and limited with blank injections (methanol) every two samples analyzed. The linearity of the in-matrix standard calibration curves for all the eleven PFAS was assessed between 0 and 40 μg L^{-1} both for nutrient solution and plant tissues (root and leaf extracts). All molecules showed good linearity, with coefficients of determination $R^2 > 0.99$ (Table S2). PFAS contents were determined using the corresponding calibration curve. Regarding wood samples, the calibration curve made for roots was used for PFAS quantification. The limit of detection (LOD) and the limit of quantification (LOQ) values were calculated for each target PFAS as the analyte peak with a signal-to-noise ratio of 3 and 10, respectively. LOD and LOQ values are reported in Table S2.

2.5. Bioconcentration factor (BCF) and translocation factor (TF)

The bioconcentration factor (*BCF*) is defined as the ratio of the concentration of PFAS in plants over the concentration of PFAS available in the medium (Chen et al., 2020). The BCF for both leaves and roots was estimated using Eq. (1), with the concentration in the biomass referred to dry weight (DW).

$$BCF = \frac{PFAS\ concentration\ in\ plant\ biomass\ (\mu g\ \ kg^{-1}\ DW)}{Initial\ PFAS\ concentration\ in\ the\ nutrient\ solution\ (\mu g\ \ L^{-1})} \quad \text{Eq. 1}$$

The translocation factor (*TF*) estimates the ability of a plant to translocate a molecule from the root system to the shoot system of the plant (Chen et al., 2020), and was calculated using Eq. (2).

$$TF = \frac{PFAS\ concentration\ in\ leaves\ (\mu g\ \ g^{-1}\ DW)}{PFAS\ concentration\ in\ roots\ (\mu g\ \ g^{-1}\ DW)} \quad \text{Eq. 2}$$

2.6. Root morphology and relative water content in roots and leaves

Three morphologically similar replicates per group were selected for radicle imaging and analysis at the end of the treatment. Root samples were scanned with a resolution of 157.5 dot/cm (400 dpi) using an EPSON Expression 11000 XL PRO scanning system. Scanned images were further analyzed with WinRHIZO software v. 5.0, to determine the total root length (cm), the average root diameter (mm) and the average root surface (cm^2). The total length and the average diameter of the roots were calculated according to Ebinezer et al. (2022): *Length = (No. of pixels in the radical skeleton/Image resolution)*; *Diameter = [(Projected area pixels/Total skeleton length pixels)] × (1/Image resolution)*. Fresh (*FW*) and dry (*DW*) weights of the roots and leaves were determined at the end of the experimental exposure. Roots and leaves samples were oven-dried at 60 °C to a constant weight in order to calculate the percentage of relative water content (*RWC*), as follows: *RWC = 100 – (DW/FW × 100)*.

2.7. Stomatal conductance

Stomatal conductance (g_{sw}) measurements were performed at the end of the PFAS exposure on a subset of plants that showed uniform growth (n = 8) from both control and treated groups with an open flow-through differential porometer (LI-600, Li-Cor Inc., USA). For each

sample, g_{sw} was measured between 11:00 and 14:00 h on 5 fully expanded leaves.

2.8. Phytohormones extraction and quantification by LC-MS/MS analysis

Phytohormones were extracted from fresh leaves using a 10% acetonitrile (ACN)/1% acetic acid cold aqueous solution. 150 mg of fresh leaf tissue were finely ground with liquid nitrogen, then the extraction buffer was added in a 1:5 ratio and vortexed for 1 min. Samples were incubated on ice with shaking for 15 min and sonicated for 15 min, keeping the water bath cold with ice. Then, samples were centrifuged at 18,400×*g* for 10 min at 4 °C and supernatants were transferred in a new tube. The extraction was repeated twice with the resultant pellets, using the same extraction buffer. Supernatants were finally filtered with 0.22 μm polyvinylidene fluoride (PVDF) membranes and the eluted volumes were measured. Samples were frozen in liquid nitrogen, dried in a lyophilizer and stored at −20 °C until LC-MS/MS analysis. Dry samples were initially resuspended in 20% ACN and then diluted to a final 0.5× concentration in 10% ACN before injection.

The amount of ABA and SA in leaves was measured by targeted LC-MS/MS analysis using the instrument previously described. Instrumental conditions are reported in Text S1, and the optimized parameters for SRM transitions are reported in Table S3. The linearity of the in-matrix standard calibration curves used for phytohormones quantification was assessed between 0 and 50 μg L^{-1}. All molecules showed a good linearity, with coefficients of determination $R^2 > 0.99$ (Table S4). LOD and LOQ values were calculated for each target molecule as the analyte peak with a signal-to-noise ratio of 3 and 10, respectively, and are reported in Table S4.

2.9. Xylem vulnerability to cavitation

Vulnerability curves (*VCs*) of six control and six PFAS-exposed plants were assessed using the air-injection technique (Rosner et al., 2019). Each sample plant was immersed in water, where both the ends of the willow cutting were progressively cut to obtain a stem sample of ~25 cm. Stem segments were debarked and trimmed under water with a sharp razor blade to a length of ~20 cm (i.e., $L > 1.5 \times VL_{MAX}$, where the estimated maximum vessel length was $VL_{MAX} = 15$ cm (estimated with the air injection technique, as described by Ewers & Fisher (1989)), and connected to a reservoir containing distilled water (at 95 cm height). Hydraulic conductance (*K*) was measured gravimetrically at 8 kPa by collecting sap at the distal end using a flow meter sensor (SLI-2000, Sensirion, Switzerland). First, *K* of fresh sample (K_{fresh}) was measured. For each sample, the maximum *K* (K_{max}) was measured after flushing with distilled water at high pressure (~0.2 MPa) for 15 min to remove possible native embolisms and given an additional 20 min to equilibrate in water. Next, samples were inserted into a double-ended pressure sleeve (PMS Instruments, USA) and subjected to a pressure of 0.5 MPa for 1 min (Rosner et al., 2019). Samples were then allowed to equilibrate in water for 20 min, and the hydraulic conductivity (K_i) was measured again as described above. This process was repeated at increasing pressures, and the percent loss of conductance (*PLC*) was then calculated using Eq. (3).

$$PLC = \left(1 - \frac{K_i}{K_{max}}\right) \times 100 \qquad \text{Eq. 3}$$

where K_i is the sample conductance measured after the *i*-step of pressurization. The pressure (*P*) applied in subsequent air injection cycles was gradually increased by steps of 0.5 MPa until 4 MPa was reached. *VCs* were obtained by fitting *PLC* vs. *-P* data using the fitplc package for R software (Duursma and Choat, 2017). The *P50* values (i.e., the water potential (-P) corresponding to *PLC* = 50%) and their 95%-confidence intervals (95%-CI) were then extracted from the VCs. Not overlapping 95%-CI between control and PFAS-exposed samples indicated a significant difference between groups.

2.10. Statistical analysis

Statistical analysis was carried out with R software v. 2022.12.0 (R Development Core RStudio Team, 2020), and differences were considered significant at $p \leq 0.05$. Potential outliers were tested by Grubbs' test and removed from the dataset prior to further statistical analyses. Root morphology data were analyzed by Mann-Whitney-Wilcoxon *U* test due to limited sample size. RWC, stomatal conductance and phytohormones content were tested by Student's test, after checking homoscedasticity by Levene's test and normality by Shapiro-Wilk test. Graphs were constructed using the ggplot2 package for R. PFAS not detected in any of the replicates are reported as < LOD.

3. Results and discussion

3.1. PFAS uptake, bioaccumulation and translocation

To evaluate the ability of willow plants to uptake PFAS substances and to confirm that all PFAS remained available throughout the experimental duration, we first analyzed the residual nutrient solution of each sample at the end of the treatment (8 days). We detected all the PFAS in the nutrient solution at the end of the experiment (Table S5), indicating that the PFAS remained available for the plants to uptake throughout the experimental duration. Taking into consideration that some amount of PFAS could be non-specifically adsorbed, these values indicate that the plants were able to uptake all the PFAS compounds from the nutrient solution in different quantities (Table S5). In particular, short chain molecules (C < 8) were found in a relatively higher amount (up to approximately 90%, with the only exception of PFBA (68%)), compared to long chain ones (C ≥ 8), (ranging from almost 40%–75%). An increasing trend in PFAS uptake as a function of the chain length can be noticed. Moreover, the presence of a sulfonic group led to a different behavior with respect to a carboxylic group for the same chain length (PFBA vs. PFBS, PFOA vs. PFOS). The amount of PFDoA in the residual nutrient solution was too low to be accurately quantified, thus it was not possible to estimate the % of residual PFDoA in a reliable manner.

The amount of PFAS substances detected in plant tissues (Fig. 1, Table S6) was consistent with the trend observed in the PFAS uptake from the nutrient solution. Regarding roots (Fig. 1A), an increasing trend in the concentrations of PFAS dependent on the increasing carbon chain length was clearly visible. Short chain molecules were detected in lower amounts compared to long chain PFAS, and a difference due to the polar group was observed. In particular, perfluoroalkyl sulfonic acids (PFSA, e.g., PFBS and PFOS in our study) accumulated more in root tissue than their equivalent molecules with a carboxylic group (PFCA - perfluoroalkyl carboxylic acids).

PFAS quantification in leaves (Fig. 1B) showed an opposite trend with respect to roots. PFBA and PFPeA stood out from all the other compounds, indicating their ability to translocate from roots. Conversely, the longest molecules (PFUnA and PFDoA) were detected in a very low amount. The presence of a sulfonic group in PFBS and PFOS limited the translocation to leaf tissues compared to PFBA and PFOA, respectively. The evaluation of PFAS quantities in plant tissues highlighted a clear trend of accumulation that is directly related to the chemical structure of the analyzed perfluorinated compounds. In particular, short chain molecules accumulated more in the leaves, whilst the long chain compounds were more abundant in the roots. Our observations on PFAS accumulation in roots and leaves were consistent with the available literature evidence on PFAS uptake in different plant species (Sharma et al., 2020; Ebinezer et al., 2022; Gredelj et al., 2020; Ghisi et al., 2019; Felizeter et al., 2012).

Although previously PFAS have been reported to accumulate in leaves and roots, our analysis of the treated stem samples, surprisingly for the first time, revealed the presence of some PFAS probably adsorbed

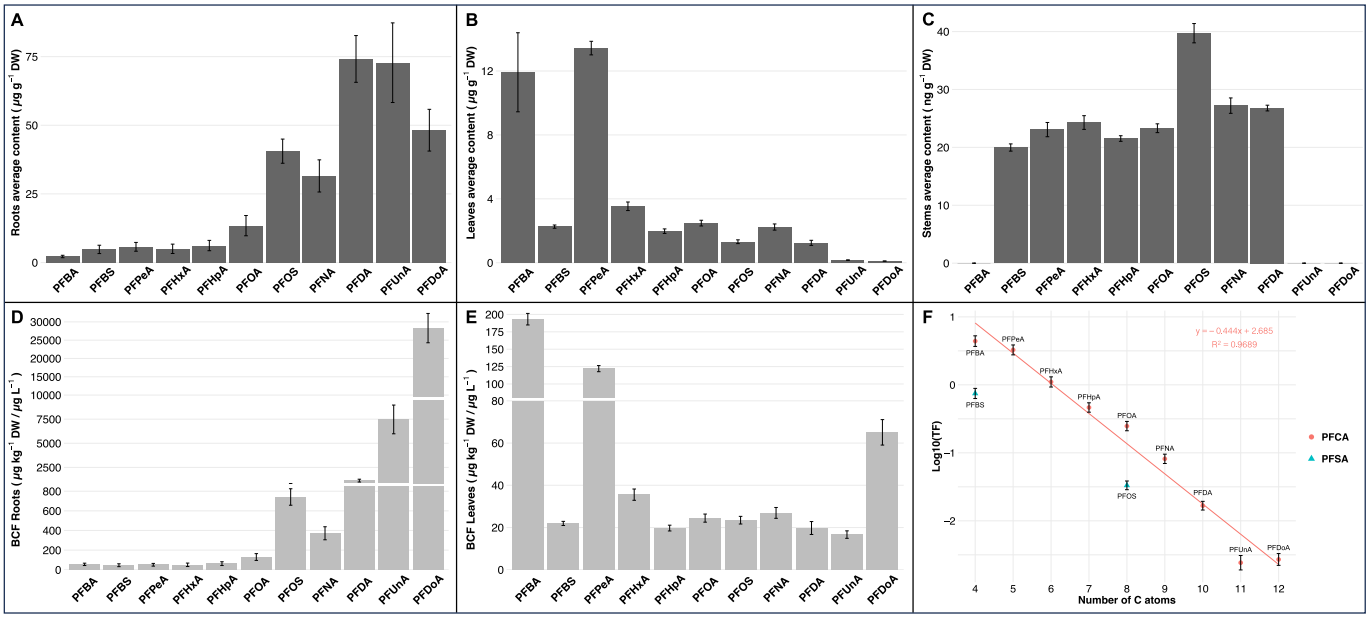

Fig. 1. Amount of PFAS compounds (expressed as μg g^{-1} DW) quantified in treated roots **(A)** and leaves **(B)** at the end of the experimental period (n = 18). **C)** PFAS content in woody stems expressed in ng g^{-1} DW (n = 6). No PFAS were detected in control samples. **D, E)** PFAS bioconcentration factor calculated for roots and leaves, respectively. **F)** Correlation between the PFAS carbon chain length and translocation factor. In all plots, values indicate mean ± standard error.

to the woody stem tissue (Fig. 1C). Compounds with chain length between 4 and 10 carbon atoms were detected (with the only exception of PFBA), however, in amounts almost 100 times lower than those observed in leaf tissues. PFUnA and PFDoA were not detected in the stem. Short chain PFCA accumulated in similar quantities, ranging from 20 up to 24 ng g^{-1} DW. PFNA and PFDA were found in slightly larger amounts (around 27 ng g^{-1} DW). PFOS showed the highest amount (39 ng g^{-1} DW), which is almost twice the PFOA quantity, indicating again the different behavior between PFCA and PFSA with the same chain length. This was also observed with PFBA and PFBS. The presence of most PFAS molecules except PFBA in the stem suggests that the latter is too hydrophilic to be retained in the wood, whereas it positively translocates to the leaves. We could not detect the longer chain PFUnA and PFDoA in the stem. It seems therefore puzzling why they are not found in woody samples, whereas they were clearly detected in leaves.

All PFAS were supplied in the same initial amount, thus allowing a direct comparison of their accumulation and translocation rate. To estimate the bioaccumulation capacity of each PFAS, we calculated the bioconcentration factors (BCF) for both roots and leaves (Fig. 1D and E; Table S6). As for PFAS content, an opposite trend for BCF in roots and leaves depending on the carbon chain length and presence of carboxylic or sulfonic group was observed. Long chain compounds were highly bioaccumulative in roots (Fig. 1D), whose BCF values range from about 1100 (PFDA), to more than 28000 μg kg^{-1} DW/μg L^{-1} (PFDoA), while BCF values of short chain molecules vary from about 46 (PFBS) to 62 μg kg^{-1} DW/μg L^{-1} (PFHpA). Similar trends have been already described in the literature, as reviewed by Lesmeister et al. (2021).

Concerning leaves (Fig. 1E), PFAS with the shortest carbon chain, like PFBA and PFPeA, had the highest BCF values (193 and 122 μg kg^{-1} DW/μg L^{-1}, respectively). As the carbon chain length increases (C > 6), BCF values drastically decrease. The BCF value associated with PFDoA was unexpectedly high (3–4 fold) compared to PFDA and PFUnA, while the significance of this finding is currently unknown it deserves further investigation. The sulfonic group led to a large difference in BCF values for PFBA and PFBS, with PFBA being approximately 9 times higher than PFBS, whereas it had no impact on PFOA and PFOS. Overall, these results are consistent with PFAS amounts quantified in plant tissues.

Finally, we calculated the translocation factors (TF) for each PFAS, which are reported in Table 1.

A TF larger than one indicates that a perfluoroalkyl substance bioaccumulates more in leaves rather than in roots (Gredelj et al., 2020). This is the case of carboxylic molecules up to 6 carbon atoms (PFBA, PFPeA and PFHxA), which were detected in a high amount in leaves (Fig. 1D). PFHpA, PFOA and PFNA exhibited a TF between 0.56 and 0.10, while the TF associated with longer chain molecules as PFDA, PFUnA and PFDoA was close to zero, indicating that they were able to translocate to leaves only to a very limited extent. Long chain PFAS are preferentially retained at the root level, as their hydrophobicity limits their movement by water through the xylem. In this regard, our finding that PFDoA was not measurable in the residual nutrient solution at the end of the experimental treatment does not necessarily imply that PFDoA molecules were absorbed by plants; rather, they are likely to adhere to the root surface by unspecific interactions. This could explain why PFDoA is largely restricted to the root tissue and has barely translocated to the leaves. Based on their chemical features, the entry of long chain PFAS molecules into roots is considered largely improbable, whereas it is more likely that highly hydrophobic compounds (such as PFDA, PFUnA and PFDoA), could be adsorbed by lipophilic root solids, such as lipids/proteins in membranes and cell walls, as hypothesized previously (Felizeter et al., 2012).

A special consideration must be done for sulfonated compounds, since the TF of PFBS and PFOS is almost 6- and 10- times lower than PFBA and PFOA, respectively. This suggests that the greater hydrophobicity imparted by the sulfonic group strongly decreases the translocation across the xylem. BCF values (Table S6) are coherent with the TF trend for all PFAS. We further investigated the correlation between the length of the PFAS carbon chain and the TF (converted in a logarithmic scale). A strong negative linear relationship for carboxylic perfluorinated compounds was observed (Fig. 1F), which was supported by a Pearson's correlation coefficient equal to −0.98. Sulfonated perfluoroalkyl compounds, whose TF values were much lower, showed a similar trend. Taken together our results are consistent and in good accordance with the uptake and distribution of PFAS in woody plants (Gobelius et al., 2017; Huff et al., 2020; Kirkwood et al., 2022), and showed that the uptake of PFAS up by the willow plants primarily depends on the chemical properties of the PFAS, in particular chain length

Table 1
PFAS translocation factors. Values indicate mean ± standard error (n = 18).

Molecule	PFBA	PFBS	PFPeA	PFHxA	PFHpA	PFOA	PFOS	PFNA	PFDA	PFUnA	PFDoA
TF	5.7 ± 1.0	0.9 ± 0.1	4.0 ± 0.5	1.4 ± 0.2	0.56 ± 0.07	0.30 ± 0.05	0.041 ± 0.007	0.10 ± 0.02	0.021 ± 0.004	0.0030 ± 0.0006	0.0038 ± 0.0007

and functional group.

3.2. Effects of PFAS on root morphology and physiology

PFAS especially at high concentrations have been previously shown to have an impact on the plant physiology (Lan et al., 2018; Du et al., 2020; Li et al., 2020a). In our study, no significant morphological differences were observed in leaves and roots in response to PFAS between control and treated plants after 8 days of exposure. Root scanning analysis also revealed no significant differences in total root length, average root diameter and average root surface area in PFAS-treated samples with respect to controls (Table 2). Based on the available phytotoxicity studies, generally PFAS at ng L^{-1} and μg L^{-1} levels are unlikely to cause any inhibitory and drastic physiological changes in higher plants (Li et al., 2022). However, the percentage of relative water content (RWC) of roots was slightly but significantly higher in PFAS-exposed plants, while no significant differences were detected for RWC of leaves (Table 2).

This suggests that PFAS exposure may not have a major impact on the root physiology of the willow plants in our experimental conditions, and thus re-endorses the suitability of willow plants for PFAS remediation or phytomanagement. However, we cannot exclude the impact on plant growth and physiology when exposed to longer duration and higher concentrations. Likewise, it is highly probable that the PFAS accumulation could impact the metabolism, since the RWC was significantly higher in treated plants compared to controls. Many metabolomics studies carried out on PFAS-exposed plants indicate that there are large metabolic rearrangements in primary and secondary metabolism in response to PFAS (Li et al., 2020a, 2020b, 2022). The root proteomic analysis of PFAS-treated maize plants also revealed that there was proteome level readjustment following PFAS exposure, pointing to changes in amino acid and fatty acid metabolic pathways (Ebinezer et al., 2022). Taken together, although there were no drastic changes in terms of plant physiology in PFAS-treated willow plants under our experimental conditions, large-scale metabolic rearrangements in response to PFAS accumulation cannot be definitely ruled out. The difference in RWC of roots due to PFAS exposure warrants further research.

3.3. PFAS-exposed plants showed a reduced stomatal conductance

Considering the PFAS taken up by the roots translocate via the xylem sap and ultimately accumulate in the leaves, it is likely that the PFAS accumulation could affect gas exchange parameters. Indeed, we observed that the PFAS exposed plants had a significantly reduced stomatal conductance (g_{sw}). At the end of the experimental period, PFAS-exposed plants had a significantly decreased g_{sw} (0.22 ± 0.01 mol H_2O m^{-2} s^{-1}) with respect to the control group (0.27 ± 0.02 mol H_2O m^{-2} s^{-1}). However, no significant change between control and PFAS-treated plants in terms of the consumption of nutrient solution was noticed.

Table 2
PFAS effects on root morphology (n = 6) and % relative water content (RWC) (n = 33). Values indicate mean ± standard error. * indicates significant difference ($p \leq 0.05$).

Parameter	Control (average)	Treated (average)
Root length (cm)	242 ± 51	258 ± 25
Root diameter (mm)	0.57 ± 0.12	0.81 ± 0.17
Root surface area (cm^2)	21.8 ± 4.1	24.6 ± 2.5
RWC leaves (%)	80.6 ± 0.5	80.5 ± 0.5
% RWC roots (%)	88.5 ± 0.5	90.0 ± 0.4*

g_{sw} can indicate the degree of stomatal opening/closure and thus, can be used as an indicator of plant water status. Based on the stomatal regulation of water status, plants can be classified as isohydric or anisohydric (McDowell et al., 2008). Isohydric plants tend to avoid dehydration, while anisohydric plants are tolerant to dehydration (Lavoie-Lamoureux et al., 2017). Isohydric plants such as *Salix* reduce the g_{sw} when the soil water potential decreases or as the atmospheric conditions dry to restrict excessive water loss and maintain a relatively high plant water potential. Apart from water availability, stomatal aperture is also influenced by environmental signals such as incident light intensity, ultraviolet radiation, CO_2 concentration, vapor pressure deficit (VPD), and leaf temperature.

Since the willow plants were grown in a hydroponic set-up and under controlled growth conditions, the reduced g_{sw} in treated willow plants is highly likely to be due to the PFAS accumulation and not to the water availability or the growth conditions. PFAS accumulation in leaf tissues is relatively higher compared to other plant tissues. This probably could be due to the water transport from the roots to the sub-stomatal cavities of the leaf mesophyll through xylem vessels, followed by the release of water vapor into the air, leading to the deposition of PFAS in the leaf cells. This process shows similarities with the accumulation of PFAS observed in human lungs (Pérez et al., 2013; Sørli et al., 2020) that is due to the water evaporation from lung cell surfaces during breathing. Hence, the decrease in g_{sw} we observed could be directly caused by PFAS accumulation in leaves.

Another possible explanation for reduced g_{sw} could be linked to the physical properties of PFAS. PFAS-based fire extinguishers typically form a thermal and evaporation barrier to eventually extinguish combustion. Following water evaporation, PFAS are likely to accumulate in the sub-stomatal cavities of the leaves, forming a barrier affecting the intracellular CO_2 level. Plants generally respond to intercellular CO_2 by altering g_{sw} to balance the influx of atmospheric CO_2. Tissue and cellular level distribution of PFAS in leaves and an in-depth analysis of gas exchange parameters could substantiate our hypothesis.

It is also suggested that the water transpired during growth influences the uptake and translocation of PFAS in plants (Blaine et al., 2014a, 2014b), suggesting any parameter affecting the stomatal opening can influence PFAS uptake. However, the exact mechanism underpinning the reduced g_{sw} in PFAS-treated willow plants remains elusive. While the insignificant difference in the nutrient solution consumption between treatment groups may not correlate with the reduced stomatal conductance we observed, it could be attributed to the short experimental duration. Also, the reduced stomatal conductance although statistically significant, was not large enough to be translated as an observable difference in the nutrient solution remaining at the end of the experimental period.

3.4. Effect of PFAS on phytohormones associated with stomatal conductance

Stomatal closure and thus, conductance is known to be mediated by a complex network of signaling pathways, with abscisic acid (ABA) being the major and the best-known player (Nemhauser et al., 2006; Huang et al., 2008). In addition to ABA, the guard cells mediating the stomatal closure respond to a variety of stimuli such as light, external Ca^{2+}, methyl jasmonate and salicylic acid (SA). There is strong evidence for SA-induced stomatal closure which occurs upon integration of the SA signaling with ABA signaling pathway in the guard cells via the

Ca^{2+}/Calcium-dependent protein kinase-dependent pathway (Prodhan et al., 2018). Under physiological conditions, the stomatal closure is induced by ABA upon interplay with other phytohormones leading to increased production of hydrogen peroxide (H_2O_2) which subsequently induces the NO levels. As a consequence, there are increased intracellular Ca^{2+} levels that reduce the guard cells' turgor inducing stomatal closure (Prakash et al., 2019).

The stomatal conductance (g_{sw}) was significantly decreased in PFAS-treated plants. Hence, in order to provide an explanation for the reduced g_{sw} we observed, ABA and SA content in the leaves was analyzed (Table 3), considering the stomatal conductance is largely under phytohormonal control. Unexpectedly, no significant differences were observed in the ABA and SA levels between control and treated samples; although both ABA and SA were lowered in PFAS-exposed plants. This firstly, suggests that the reduced g_{sw} we observed could be ABA- and SA-independent, but rather it could be due to a physical hindrance (caused by PFAS accumulation) affecting the stomatal conductance.

A decreased ABA concentration by at least 60% has been already reported in lettuce plants co-exposed to PFOA and PFOS (Li et al., 2020a), while no previous information about the PFAS effect on SA content is available to the best of our knowledge. Since the reduced g_{sw} we observed may not be regulated by ABA and/or SA, it is possible that PFAS-induced reactive oxygen species (ROS) could have mediated the stomatal closure. PFAS have been previously reported to induce predominantly H_2O_2 among other ROS in leaves causing oxidative stress (Li et al., 2021; Zhang et al., 2020) and one of the earliest hallmarks of stomatal closure is ROS accumulation (Singh et al., 2017). As the phytohormones (ABA and SA) are not significantly affected, we speculate that the reduced g_{sw} in PFAS-treated plants may be largely mediated by the increased ROS production, usually reported in PFAS-exposed plants (Li et al., 2022).

3.5. Impact of PFAS on xylem vulnerability to embolism

The preliminary assessment of native embolism revealed that the xylem vasculature of all samples was water-saturated. More specifically, PLC in fresh samples compared to saturated conditions followed by flushing at high pressure was always $< 15\%$ in both control and PFAS-exposed plants. Embolism generally causes a disruption of the continuum root-to-leaf water column. Isohydric plants such as *Salix* generally reduce the stomatal aperture to avoid building up of water tension in the vessels when there is a drop in the water potential (Chen et al., 2019). While the reduced g_{sw} may indicate a decreased water potential, unexpectedly no evidence for native embolism in the stems of PFAS-treated plants was found. Vulnerability curves (*VCs*) were characterized by the typical S shape, but were significantly different between control and PFAS-exposed stems (Fig. 2). In fact, the *P50* value derived from the VCs was significantly higher (i.e., less negative) in PFAS-exposed ($P50 = -2.65 \pm 0.11$ MPa) than control ($P50 = -3.12 \pm 0.13$ MPa) plants, suggesting that the PFAS-exposed stems were more vulnerable to cavitation. We have detected PFAS in the stems of treated willow plants and consistently, MS-based imaging also has revealed the distribution of PFOA and PFOS in xylem vessels (Wang et al., 2020b). Given the physico-chemical properties of PFAS, it is likely that the PFAS distributed in the xylem vessels could have altered the surface properties of the inner cell walls and caused perturbations in the hydraulic properties of the vascular system. Perfluorinated substances have been previously shown to alter membrane permeability and fluidity in animal models and can readily be incorporated into the membrane by partitioning to lipids (Zhao et al., 2023). Thus, altered xylem vessels can explain the increased vulnerability to cavitation in the hydraulic system of PFAS-treated plants we observed.

Table 3
Phytohormones content in fresh leaves determined at the end of the experimental period. Values indicate mean ± standard error (n = 33). Percentage of variation is expressed as Treated vs. Control.

Phytohormone	Control (average)	Treated (average)	% Variation	p value
Abscisic acid (ng g^{-1} FW)	76 ± 8	61 ± 5	−19.6	0.12
Salicylic acid (ng g^{-1} FW)	128 ± 11	110 ± 7	−14.1	0.16

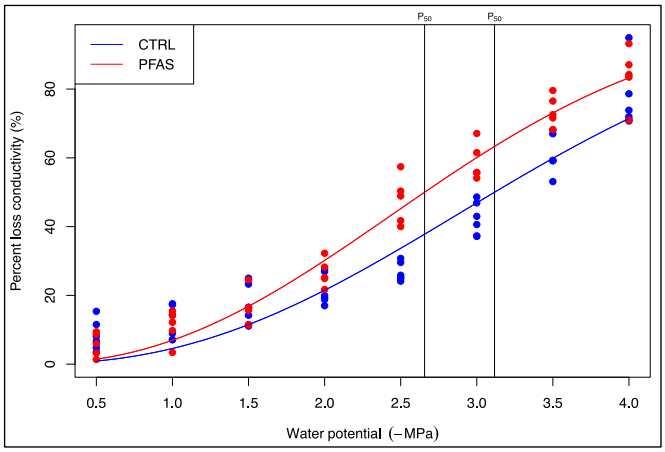

Fig. 2. Hydraulic vulnerability curves of control (n = 6) and PFAS-exposed plants (n = 6). The blue and red dots denote individual measurements. (For interpretation of the references to colour in this figure legend, the reader is referred to the Web version of this article.)

4. Conclusions

The effect of the ubiquitous and persistent PFAS on plant physiology at concentrations often detected in the environment is not fully understood. In the present study, PFAS accumulation in willow plants primarily depended on the chain length and functional groups of such chemicals. PFAS accumulation in leaves decreased the stomatal conductance, without significantly affecting the phytohormones levels and shown for the first time that PFAS occurrence in the stems increased the xylem susceptibility to air embolism. Altered stomatal conductance could be directly due to PFAS accumulation in the leaves. Increased vulnerability of treated willow plants to xylem cavitation could be linked to the PFAS accumulation in the xylem conduits that has possibly altered the surface properties and thus, water movement in the plant indirectly altering the stomatal conductance. The precise mechanisms underpinning the PFAS accumulation-induced alteration in stomatal conductance and xylem susceptibility to cavitation need to be further explored. Since we observed this in hydroponically grown plants, it needs to be confirmed if plants growing in PFAS-contaminated soil also are impacted likewise. Nevertheless, if reduced stomatal conductance and increased risk of embolism that we observed with willow plants could be surmised as a general impact on different species in the plant kingdom when exposed to PFAS, it can have larger eco-physiological implications. With the worldwide diffusion of these pollutants, an altered stomatal conductance in large terrestrial ecosystems can negatively impact efficient atmospheric CO_2 exchange and can contribute to global warming. Similarly, PFAS-exposed ecosystems with increased risk of xylem cavitation may be more vulnerable to drought episodes and drought-induced mortality due to hydraulic failure, consequently, leading to reduced yield and forest productivity. Taken together with an unprecedented increase in global temperature, drought episodes and atmospheric CO_2 burden in recent years, diffuse contamination of large ecosystems with PFAS is a serious global concern. Large-scale ecological implications of PFAS pollution are not fully understood and hence, deserve major attention from the scientific community in addition to

pushing towards understanding the impact of PFAS accumulation in plants.

CRediT authorship contribution statement

Ilaria Battisti: Investigation, Validation, Formal analysis, Visualization, Writing – original draft, Writing – review & editing. **Dario Zambonini:** Investigation, Formal analysis, Visualization, Writing – original draft. **Leonard Barnabas Ebinezer:** Writing – original draft, Writing – review & editing. **Anna Rita Trentin:** Investigation, Validation, Resources. **Franco Meggio:** Methodology, Writing – review & editing. **Giai Petit:** Methodology, Supervision, Writing – original draft, Writing – review & editing. **Antonio Masi:** Conceptualization, Methodology, Writing – review & editing, Funding acquisition, Project administration, Supervision.

Declaration of competing interest

The authors declare that they have no known competing financial interests or personal relationships that could have appeared to influence the work reported in this paper.

Data availability

Data will be made available on request.

Acknowledgments

This research was supported by the University of Padova fund BIRD223343. The Authors wish to thank the University of Padova for supporting the acquisition of the TSQ Quantiva triple quadrupole mass spectrometer instrument by 2015/CPDB15489 funding. The Authors also wish to thank Prof. Giancarlo Renella from the University of Padova for providing valuable comments during the manuscript revision. Leonard Barnabas Ebinezer was supported by a postdoctoral grant from the University of Padova. Veneto Agricoltura is gratefully acknowledged for the willow cuttings supply.

Appendix A. Supplementary data

Supplementary data to this article can be found online at https://doi.org/10.1016/j.chemosphere.2023.140380.

References

Adams, K.J., Pratt, B., Bose, N., Dubois, L.G., St John-Williams, L., Perrott, K.M., Ky, K., Kapahi, P., Sharma, V., MacCoss, M.J., Moseley, M.A., Colton, C.A., MacLean, B.X., Schilling, B., Thompson, J.W., 2020. Alzheimer's disease metabolomics consortium. Skyline for small molecules: a unifying software package for quantitative metabolomics. J. Proteome Res. 19 (4), 1447–1458. https://doi.org/10.1021/acs.jproteome.9b00640. Apr 3.

Adu, O., Ma, X., Sharma, V.K., 2023. Bioavailability, phytotoxicity and plant uptake of per-and polyfluoroalkyl substances (PFAS): a review. J. Hazard Mater. 447, 130805 https://doi.org/10.1016/j.jhazmat.2023.130805. Apr 5.

Ahrens, L., 2011. Polyfluoroalkyl compounds in the aquatic environment: a review of their occurrence and fate. J. Environ. Monit. 13 (1), 20–31. https://doi.org/10.1039/c0em00373e. Jan.

Barigah, T.S., Charrier, O., Douris, M., Bonhomme, M., Herbette, S., Améglio, T., Fichot, R., Brignolas, F., Cochard, H., 2013. Water stress-induced xylem hydraulic failure is a causal factor of tree mortality in beech and poplar. Ann. Bot. 112 (7), 1431–1437. https://doi.org/10.1093/aob/mct204. Nov.

Blaine, A.C., Rich, C.D., Sedlacko, E.M., Hundal, L.S., Kumar, K., Lau, C., Mills, M.A., Harris, K.M., Higgins, C.P., 2014a. Perfluoroalkyl acid distribution in various plant compartments of edible crops grown in biosolids-amended soils. Environ. Sci. Technol. 48 (14), 7858–7865. https://doi.org/10.1021/es500016s. Jul 15.

Blaine, A.C., Rich, C.D., Sedlacko, E.M., Hyland, K.C., Stushnoff, C., Dickenson, E.R., Higgins, C.P., 2014b. Perfluoroalkyl acid uptake in lettuce (Lactuca sativa) and strawberry (Fragaria ananassa) irrigated with reclaimed water. Environ. Sci. Technol. 48 (24), 14361–14368. https://doi.org/10.1021/es504150h. Dec 16.

Chen, C.H., Yang, S.H., Liu, Y., Jamieson, P., Shan, L., Chu, K.H., 2020. Accumulation and phytotoxicity of perfluorooctanoic acid and 2,3,3,3-tetrafluoro-2-(heptafluoropropoxy)propanoate in Arabidopsis thaliana and Nicotiana benthamiana. Environ. Pollut. 259, 113817 https://doi.org/10.1016/j.envpol.2019.113817. Apr.

Chen, Z., Liu, S., Lu, H., Wan, X., 2019. Interaction of stomatal behaviour and vulnerability to xylem cavitation determines the drought response of three temperate tree species. AoB Plants 11 (5), plz058. https://doi.org/10.1093/aobpla/plz058. Sep 23.

Cochard, H., 2006. Cavitation in trees. Comptes Rendus Physique 7, 1018–1026. https://doi.org/10.1016/j.crhy.2006.10.012.

Cook, B.I., Mankin, J.S., Anchukaitis, K.J., 2018. Climate change and drought: from past to future. Curr. Clim. Change Rep. 4, 164–179. https://doi.org/10.1007/s40641-018-0093-2. May 12.

Darrall, N.M., 1989. The effect of air pollutants on physiological processes in plants. Plant Cell Environ. 12 (1), 1–30. https://doi.org/10.1111/j.1365-3040.1989.tb01913.x. Jan.

Du, W., Liu, X., Zhao, L., Xu, Y., Yin, Y., Wu, J., Ji, R., Sun, Y., Guo, H., 2020. Response of cucumber (Cucumis sativus) to perfluorooctanoic acid in photosynthesis and metabolomics. Sci Total Environ. 724, 138257. https://doi.org/10.1016/j.scitotenv.2020.138257.

Duursma, R.A., Choat, B., 2017. Fitplc - an R package to fit hydraulic vulnerability curves. J. Plant Hydraul. 4 https://doi.org/10.20870/jph.2017.e002.

Ebinezer, L.B., Battisti, I., Sharma, N., Ravazzolo, L., Ravi, L., Trentin, A.R., Barion, G., Panozzo, A., Dall'Acqua, S., Vamerali, T., Quaggiotti, S., Arrigoni, G., Masi, A., 2022. Perfluorinated alkyl substances affect the growth, physiology and root proteome of hydroponically grown maize plants. J. Hazard Mater. 438, 129512 https://doi.org/10.1016/j.jhazmat.2022.129512. Sep 15.

Evangelou, M.W.H., Robinson, B.H., 2022. The phytomanagement of PFAS-contaminated land. Int. J. Environ. Res. Publ. Health 19 (11), 6817. https://doi.org/10.3390/ijerph19116817. Jun 2.

Ewers, F.W., Fisher, J.B., 1989. Techniques for measuring vessel lengths and diameters in stems of woody plants. Am. J. Bot. 76 (5), 645–656. https://doi.org/10.1002/j.1537-2197.1989.tb11360.x. May 01.

Felizeter, S., McLachlan, M.S., de Voogt, P., 2012. Uptake of perfluorinated alkyl acids by hydroponically grown lettuce (Lactuca sativa). Environ. Sci. Technol. 46 (21), 11735–11743. https://doi.org/10.1021/es302398u. Nov 6.

Fenton, S.E., Ducatman, A., Boobis, A., DeWitt, J.C., Lau, C., Ng, C., Smith, J.S., Roberts, S.M., 2021. Per- and Polyfluoroalkyl Substance Toxicity and Human Health Review: Current State of Knowledge and Strategies for Informing Future Research. Environ. Toxicol. Chem. 40 (3), 606–630. https://doi.org/10.1002/etc.4890.

Ghisi, R., Vamerali, T., Manzetti, S., 2019. Accumulation of perfluorinated alkyl substances (PFAS) in agricultural plants: a review. Environ. Res. 169, 326–341. https://doi.org/10.1016/j.envres.2018.10.023. Feb.

Gobelius, L., Lewis, J., Ahrens, L., 2017. Plant uptake of per- and polyfluoroalkyl substances at a contaminated fire training facility to evaluate the phytoremediation potential of various plant species. Environ. Sci. Technol. 51 (21), 12602–12610. https://doi.org/10.1021/acs.est.7b02926. Nov 7.

Gredelj, A., Nicoletto, C., Polesello, S., Ferrario, C., Valsecchi, S., Lava, R., Barausse, A., Zanon, F., Palmeri, L., Guidolin, L., Bonato, M., 2020. Uptake and translocation of perfluoroalkyl acids (PFAAs) in hydroponically grown red chicory (Cichorium intybus L.): Growth and developmental toxicity, comparison with growth in soil and bioavailability implications. Sci. Total Environ. 720, 137333. https://doi.org/10.1016/j.scitotenv.2020.137333.

Grossiord, C., Buckley, T.N., Cernusak, L.A., Novick, K.A., Poulter, B., Siegwolf, R.T.W., Sperry, J.S., McDowell, N.G., 2020. Plant responses to rising vapor pressure deficit. New Phytol. 226 (6), 1550–1566. https://doi.org/10.1111/nph.16485. Jun.

Hoagland, D.R., 1933. Nutrition of Strawberry Plant under Controlled Conditions. (A) Effects of Deficiencies of Boron and Certain Other Elements,(b) Susceptibility to Injury from Sodium Salts. Proc. American Society of Horticulture Science, vol. 30, pp. 288–294.

Huang, D., Wu, W., Abrams, S.R., Cutler, A.J., 2008. The relationship of drought-related gene expression in Arabidopsis thaliana to hormonal and environmental factors. J. Exp. Bot. 59 (11), 2991–3007. https://doi.org/10.1093/jxb/ern155.

Huff, D.K., Morris, L.A., Sutter, L., Costanza, J., Pennell, K.D., 2020. Accumulation of six PFAS compounds by woody and herbaceous plants: potential for phytoextraction. Int. J. Phytoremediation 22 (14), 1538–1550. https://doi.org/10.1080/15226514.2020.1786004.

Kirkwood, K.I., Fleming, J., Nguyen, H., Reif, D.M., Baker, E.S., Belcher, S.M., 2022. Utilizing pine needles to temporally and spatially profile per- and polyfluoroalkyl substances (PFAS). Environ. Sci. Technol. 56 (6), 3441–3451. https://doi.org/10.1021/acs.est.1c06483. Mar 15.

Lan, Z., Zhou, M., Yao, Y., Sun, H., 2018. Plant uptake and translocation of perfluoroalkyl acids in a wheat-soil system. Environ. Sci. Pollut. Res. Int. 25 (31), 30907–30916. https://doi.org/10.1007/s11356-018-3070-3.

Lavoie-Lamoureux, A., Sacco, D., Risse, P.A., Lovisolo, C., 2017. Factors influencing stomatal conductance in response to water availability in grapevine: a meta-analysis. Physiol Plant 159 (4), 468–482. https://doi.org/10.1111/ppl.12530. Apr;.

Lens, F., Gleason, S.M., Bortolami, G., Brodersen, C., Delzon, S., Jansen, S., 2022. Functional xylem characteristics associated with drought-induced embolism in angiosperms. New Phytol. 236 (6), 2019–2036. https://doi.org/10.1111/nph.18447. Dec.

Lesmeister, L., Lange, F.T., Breuer, J., Biegel-Engler, A., Giese, E., Scheurer, M., 2021. Extending the knowledge about PFAS bioaccumulation factors for agricultural plants - a review. Sci. Total Environ. 766, 142640 https://doi.org/10.1016/j.scitotenv.2020.142640.

Li, P., Oyang, X., Xie, X., Guo, Y., Li, Z., Xi, J., Zhu, D., Ma, X., Liu, B., Li, J., Xiao, Z., 2020a. Perfluorooctanoic acid and perfluorooctane sulfonate co-exposure induced

changes of metabolites and defense pathways in lettuce leaves. Environ. Pollut. 256, 113512 https://doi.org/10.1016/j.envpol.2019.113512.
Li, P., Oyang, X., Xie, X., Li, Z., Yang, H., Xi, J., Guo, Y., Tian, X., Liu, B., Li, J., Xiao, Z., 2020b. Phytotoxicity induced by perfluorooctanoic acid and perfluorooctane sulfonate via metabolomics. J. Hazard Mater. 389, 121852 https://doi.org/10.1016/j.jhazmat.2019.121852. May 5.
Li, J., Sun, J., Li, P., 2022. Exposure routes, bioaccumulation and toxic effects of per- and polyfluoroalkyl substances (PFASs) on plants: a critical review. Environ. Int. 158, 106891 https://doi.org/10.1016/j.envint.2021.106891. Jan.
Li, P., Xiao, Z., Xie, X., Li, Z., Yang, H., Ma, X., Sun, J., Li, J., 2021. Perfluorooctanoic acid (PFOA) changes nutritional compositions in lettuce (Lactuca sativa) leaves by activating oxidative stress. Environ. Pollut. 285, 117246 https://doi.org/10.1016/j.envpol.2021.117246. Sep 15.
Marx, W., Haunschild, R., Bornmann, L., 2021. Heat waves: a hot topic in climate change research. Theor. Appl. Climatol. 146 (1–2), 781–800. https://doi.org/10.1007/s00704-021-03758-y.
McDowell, N., Pockman, W.T., Allen, C.D., Breshears, D.D., Cobb, N., Kolb, T., Plaut, J., Sperry, J., West, A., Williams, D.G., Yepez, E.A., 2008. Mechanisms of plant survival and mortality during drought: why do some plants survive while others succumb to drought? New Phytol. 178 (4), 719–739. https://doi.org/10.1111/j.1469-8137.2008.02436.x.
Nardini, A., Salleo, S., Jansen, S., 2011. More than just a vulnerable pipeline: xylem physiology in the light of ion-mediated regulation of plant water transport. J. Exp. Bot. 62 (14), 4701–4718. https://doi.org/10.1093/jxb/err208.
Nemhauser, J.L., Hong, F., Chory, J., 2006. Different plant hormones regulate similar processes through largely nonoverlapping transcriptional responses. Cell 126 (3), 467–475. https://doi.org/10.1016/j.cell.2006.05.050.
Pérez, F., Nadal, M., Navarro-Ortega, A., Fàbrega, F., Domingo, J.L., Barceló, D., Farré, M., 2013. Accumulation of perfluoroalkyl substances in human tissues. Environ. Int. 59, 354–362. https://doi.org/10.1016/j.envint.2013.06.004. Sep.
Prakash, V., Singh, V.P., Tripathi, D.K., Sharma, S., Corpas, F.J., 2019. Crosstalk between nitric oxide (NO) and abscisic acid (ABA) signalling molecules in higher plants. Environ. Exp. Bot. 161, 41–49. https://doi.org/10.1016/j.envexpbot.2018.10.033. May.
Prodhan, M.Y., Munemasa, S., Nahar, M.N., Nakamura, Y., Murata, Y., 2018. Guard cell salicylic acid signaling is integrated into abscisic acid signaling via the Ca2+/CPK-dependent pathway. Plant Physiol. 178 (1), 441–450. https://doi.org/10.1104/pp.18.00321.
Rai, P.K., 2016. Impacts of particulate matter pollution on plants: implications for environmental biomonitoring. Ecotoxicol. Environ. Saf. 129 (120), 36. https://doi.org/10.1016/j.ecoenv.2016.03.012.
Rosner, S., Heinze, B., Savi, T., Dalla-Salda, G., 2019. Prediction of hydraulic conductivity loss from relative water loss: new insights into water storage of tree stems and branches. Physiol Plant 165 (4), 843–854. https://doi.org/10.1111/ppl.12790.
RStudio Team, 2020. RStudio: Integrated Development for R. RStudio. PBC, Boston, MA. http://www.rstudio.com/.
Sharma, N., Barion, G., Shrestha, I., Ebinezer, L.B., Trentin, A.R., Vamerali, T., Mezzalira, G., Masi, A., Ghisi, R., 2020. Accumulation and effects of perfluoroalkyl substances in three hydroponically grown Salix L. species. Ecotoxicol. Environ. Saf. 191, 110150 https://doi.org/10.1016/j.ecoenv.2019.110150. Mar 15.
Singh, R., Parihar, P., Singh, S., Mishra, R.K., Singh, V.P., Prasad, S.M., 2017. Reactive oxygen species signaling and stomatal movement: current updates and future perspectives. Redox Biol. 11, 213–218. https://doi.org/10.1016/j.redox.2016.11.006. Apr.
Sørli, J.B., Låg, M., Ekeren, L., Perez-Gil, J., Haug, L.S., Da Silva, E., Matrod, M.N., Gützkow, K.B., Lindeman, B., 2020. Per- and polyfluoroalkyl substances (PFASs) modify lung surfactant function and pro-inflammatory responses in human bronchial epithelial cells. Toxicol. Vitro 62, 104656. https://doi.org/10.1016/j.tiv.2019.104656. Feb.
Sunderland, E.M., Hu, X.C., Dassuncao, C., Tokranov, A.K., Wagner, C.C., Allen, J.G., 2019. A review of the pathways of human exposure to poly- and perfluoroalkyl substances (PFASs) and present understanding of health effects. J. Expo. Sci. Environ. Epidemiol. 29 (2), 131–147. https://doi.org/10.1038/s41370-018-0094-1. Mar.
Valsecchi, S., Rusconi, M., Mazzoni, M., Viviano, G., Pagnotta, R., Zaghi, C., Serrini, G., Polesello, S., 2015. Occurrence and sources of perfluoroalkyl acids in Italian river basins. Chemosphere 129, 126–134. https://doi.org/10.1016/j.chemosphere.2014.07.044. Jun.
Vasić, V., Kukić, D., Šćiban, M., Đurišić-Mladenović, N., Velić, N., Pajin, B., Crespo, J., Farre, M., Šereš, Z., 2023. Lignocellulose-based biosorbents for the removal of contaminants of emerging concern (CECs) from water: a review. Water 15 (10), 1853. https://doi.org/10.3390/w15101853.
Wang, Q., Tsui, M.M.P., Ruan, Y., Lin, H., Zhao, Z., Ku, J.P.H., Sun, H., Lam, P.K.S., 2019. Occurrence and distribution of per- and polyfluoroalkyl substances (PFASs) in the seawater and sediment of the South China sea coastal region. Chemosphere 231, 468–477. https://doi.org/10.1016/j.chemosphere.2019.05.162. Sep.
Wang, W., Rhodes, G., Ge, J., Yu, X., Li, H., 2020a. Uptake and accumulation of per- and polyfluoroalkyl substances in plants. Chemosphere 261, 127584. https://doi.org/10.1016/j.chemosphere.2020.127584. Dec.
Wang, T.T., Ying, G.G., Shi, W.J., Zhao, J.L., Liu, Y.S., Chen, J., Ma, D.D., Xiong, Q., 2020b. Uptake and translocation of perfluorooctanoic acid (PFOA) and perfluorooctanesulfonic acid (PFOS) by wetland plants: tissue- and cell-level distribution visualization with desorption electrospray ionization mass spectrometry (DESI-MS) and transmission electron microscopy equipped with energy-dispersive spectroscopy (TEM-EDS). Environ. Sci. Technol. 54 (10), 6009–6020. https://doi.org/10.1021/acs.est.9b05160. May 19.
Würth, A., Mechler, M., Menberg, K., Ikipinar, M.A., Martus, P., Söhlmann, R., Boeddinghaus, R.S., Blum, P., 2023. Phytoscreening for per- and polyfluoroalkyl substances at a contaminated site in Germany. Environ. Sci. Technol. 57 (10), 4122–4132. https://doi.org/10.1021/acs.est.2c04519.
Xu, B., Qiu, W., Du, J., Wan, Z., Zhou, J.L., Chen, H., Liu, R., Magnuson, J.T., Zheng, C., 2022. Translocation, bioaccumulation, and distribution of perfluoroalkyl and polyfluoroalkyl substances (PFASs) in plants. iScience 25 (4), 104061. https://doi.org/10.1016/j.isci.2022.
Yang, X., Ye, C., Liu, Y., Zhao, F.J., 2015. Accumulation and phytotoxicity of perfluorooctanoic acid in the model plant species Arabidopsis thaliana. Environ. Pollut. 206, 560–566. https://doi.org/10.1016/j.envpol.2015.07.050. Nov.
Zhang, D.Q., Wang, M., He, Q., Niu, X., Liang, Y., 2020. Distribution of perfluoroalkyl substances (PFASs) in aquatic plant-based systems: from soil adsorption and plant uptake to effects on microbial community. Environ. Pollut. 257, 113575 https://doi.org/10.1016/j.envpol.2019.113575. Feb.
Zhao, L., Teng, M., Zhao, X., Li, Y., Sun, J., Zhao, W., Ruan, Y., Leung, K.M.Y., Wu, F., 2023. Insight into the binding model of per- and polyfluoroalkyl substances to proteins and membranes. Environ. Int. 175, 107951 https://doi.org/10.1016/j.envint.2023.107951. May.
Zhou, Y., Zhou, Z., Lian, Y., Sun, X., Wu, Y., Qiao, L., Wang, M., 2021. Source, transportation, bioaccumulation, distribution and food risk assessment of perfluorinated alkyl substances in vegetables: a review. Food Chem. 349, 129137 https://doi.org/10.1016/j.foodchem.2021.129137. Jul 1.

Glossary

ABA: abscisic acid
ACN: acetonitrile
ASE: accelerated solvent extraction
BCF: bioconcentration factor
CA: cellulose acetate
DW: dry weight
FW: fresh weight
g_{sw}*:* stomatal conductance
K: sample hydraulic conductance
K_{fresh}*:* hydraulic conductance of fresh sample
K_{max}*:* maximum sample hydraulic conductance
LC-MS/MS: liquid chromatography tandem mass spectrometry
LOD: limit of detection
LOQ: limit of quantification
P: pressure
PAR: photosynthetic active radiation
PFAS: poly- and perfluoroalkyl substances
PFBA: perfluorobutanoic acid
PFBS: perfluorobutane sulfonate
PFCA: perfluoroalkyl carboxylic acids
PFDA: perfluorodecanoic acid
PFDoA: perfluorododecanoic acid
PFHxA: perfluorohexanoic acid
PFHpA: perfluoroheptanoic acid
PFNA: perfluorononanoic acid
PFOA: perfluorooctanoic acid
PFOS: perfluorooctane sulfonate
PFPeA: perfluoropentanoic acid
PFSA: perfluoroalkyl sulfonic acids
PFUnA: perfluoroundecanoic acid
PLC: percent loss of conductivity
PVDF: polyvinylidene fluoride
ROS: reactive oxygen species
RWC: relative water content
SA: salicylic acid
SRM: selected reaction monitoring
TF: translocation factor
VC: vulnerability curve
VL_{MAX}*:* maximum vessel length
VPD: vapor pressure deficit